IEEE Copyright Notice

Date of publication: December 17, 2022

DOI: 10.1109/TIA.2022.3232468

*The final publication of this paper is cited as:
H. Yamasaki, H. Yamamoto, Y. Koizumi, Y. Fukuda, T. Kuroki and M. Okubo, Dry Emission Control Technology for Glass Melting Furnace by Plasma-Chemical Hybrid Processing, IEEE Transactions on Industry Applications, vol. 59, no. 2, pp. 2421-2429, March-April 2023.

Dry Emission Control Technology for Glass Melting Furnace by Plasma-Chemical Hybrid Processing*

Haruhiko Yamasaki
Member, IEEE
Department of Mechanical Engineering
Osaka Metropolitan University
1-1 Gakuen-cho, Naka-ku, Sakai
599-8531, Japan
hyamasaki@omu.ac.jp

Hashira Yamamoto
Environmental Affairs Office,
Nihon Yamamura Glass Co., Ltd.,
15-1 Nishimukojima-cho,
Amagasaki, Hyogo 660-8580,
Japan
(Concurrent affiliation) Osaka Metropolitan University
yamamoto_h3@yamamura.co.jp

Yuki Koizumi
Department of Mechanical Engineering
Osaka Prefecture University
1-1 Gakuen-cho, Naka-ku, Sakai
599-8531, Japan
cyhuhkoii@gmail.com

Yuta Fukuda
Department of Mechanical Engineering
Osaka Prefecture University
1-1 Gakuen-cho, Naka-ku, Sakai
599-8531, Japan
fuyu.sab03100@gmail.com

Tomoyuki Kuroki
Member, IEEE
Department of Mechanical Engineering
Osaka Prefecture University
1-1 Gakuen-cho, Naka-ku, Sakai
599-8531, Japan
kuroki@omu.ac.jp

Masaaki Okubo
Senior Member, IEEE
Department of Mechanical Engineering
Osaka Metropolitan University
1-1 Gakuen-cho, Naka-ku, Sakai
599-8531, Japan
mokubo@mokubo.com

***Abstract* -- To use the continuous combustion of fossil fuels as a sustainable energy source, a low-cost and energy-saving exhaust gas treatment for NO_x, SO_x, and suspended particulate matter is required. The plasma hybrid exhaust gas treatment technology proposed by the authors is not only a method of plasma treatment, but also a method that combines it with a chemical process, such as chemical solution stabilizer, to clean exhaust gas. This study reports the simulation and application of glass melting furnace exhaust gas treatment as a practical result of the plasma chemical hybrid process (PCHP). In the experiment, higher removal efficiencies of NO, NO_x, and SO_x (33, 16, and 55%, respectively) were obtained. The energy efficiency of NO_x removal by evaluating the electrical power using the cost of NaOH and the power of ozonizers was measured to be 23 g(NO_2)/kWh. From comparison, the simulated and experimental temperature distributions and NO_x concentration were found to be in good agreements. This indicates that numerical design simulation produces a satisfactory result. PCHP can potentially be the most suitable method for exhaust gas treatment in glass melting furnaces.**

***Index Terms*-- Nonthermal plasma, Dielectric barrier discharge, Dry emission control, Glass melting furnace, Plasma-chemical process, NO_x, SO_x**

I. Introduction

The recent increase in the fossil fuel combustion rate in the energy supply has changed the Japanese domestic environmental protection and energy situation. Due to the shutdown of nuclear power plants in recent years, the amount of power generated by thermal power generation plants of electric power companies has increased to approximately 75% of the total power generated in 2020, and the importance of the thermal power generation has been growing. Moreover, in recent years, the new construction of liquefied natural gas (LNG) gas turbine combined cycle (GTCC) power plants has increased; however, there are plans to build lower-cost coal-fired power plants. Notably, the boilers used for heating and cooling at a district level, such as those in schools, hospitals, hotels, and factories, are switching to city gas. Meanwhile, the regulation values based on the air pollution control law and local regulations have become stricter; however, this situation has changed in recent years.

The main components of fossil fuels are carbon (C), hydrogen (H), sulfur (S), and nitrogen (N). However, carbon oxides (CO and CO_2), sulfur oxides (SO_x, main components SO_2 and SO_3), nitrogen oxides (NO_x, main components NO and NO_2), particulate matter (PM, main components fly ash and dust), and hydrocarbons (HCs) in the atmosphere generated by the combustion of fossil fuels pollute the environment. Of these harmful components, SO_x is pre-desulfurized (sulfur, S, is removed from the fuel) or treated by flue gas desulfurization with calcium carbonate aqueous solution (SO_x is removed with wet lime gypsum), and PM is filtered using a bag filter (BF) or an electrostatic precipitator (EP). As a result, technologies for preventing the release of SO_x and PM to the atmosphere have been almost completely established. At present, the major issues in developed countries include the emission of NO_x, which causes photochemical

smog, health hazards, and acid rain, becomes a precursor of $PM_{2.5}$, and CO_2 which causes global warming.

The concentration of NO_x in exhaust gas is typically several tens to several hundred ppm. In many thermal power plants and regional waste disposal plant combustion furnaces, NO_x reduction (denitration or De-NO_x) is performed using the selective catalytic reduction (SCR) method. In this method, the exhaust gas passes through a vanadium oxide catalyst (V_2O_5) or copper (II) oxide (CuO) installed in the reactor, and ammonia gas is injected upstream of the catalyst. This is an effective De-NO_x technology. However, the operational cost is relatively high. Moreover, an exhaust gas temperature of 300°C is required to activate the catalyst. In a waste combustion furnace, the exhaust gas temperature of the SCR catalyst does not reach this level due to the process that prevents dioxin emission, and the temperature of the exhaust gas is raised by a heater or an equivalent device, which requires additional energy. In addition, small and medium-sized combustion furnace boilers, which are typically used in regionally distributed energy supply systems, are widely used for industrial steam/hot water supply, district heating/cooling, and hot water supply, etc., and are indispensable and play a significant role in our daily lives. At present, ammonia, which is a hazardous substance, is unsafe for use, and the aftertreatment of NO_x exhaust gas has not been performed yet. We believe that the plasma hybrid aftertreatment described here is a promising means of De-NO_x, having low energy consumption for these thermal power plants, waste treatment plant combustion furnaces, and small- and medium-sized combustion furnace boilers [1]–[7].

A low-cost and energy-saving NO_x, SO_x, PM, and CO_2 exhaust gas treatment is necessary to enable the continued use of fossil and biofuel combustion as a full-fledged energy source. The recently proposed plasma chemical hybrid exhaust gas cleaning technology avoids the problems of the catalytic method by using a technique that combines plasma with a chemical solution process for exhaust gas cleaning instead of using plasma alone. It is a novel processing technology that can significantly reduce the use of plasma energy. Moreover, it is expected to provide an innovative global environmental protection system for boilers, diesel vehicles, marine diesel engines, industrial incinerators, and diesel generators [8]–[26].

This study reports the application results of plasma hybrid aftertreatment technology on glass melting furnace exhaust gas treatment [27]–[30] performed by Osaka Prefecture University in collaboration with Nihon Yamamura Glass Co. Ltd,. It is difficult to apply the SCR for De-NO_x [31]–[33] due to the corrosive impurities contained in the exhaust gas of the glass manufacturing system (glass melting furnace). Because the SCR cannot be applied, there was almost no effective De-NO_x aftertreatment method. Osaka Prefecture University has been conducting joint research with Nihon Yamamura Glass Co., Ltd. of Japan with the intention to apply the plasma and chemical hybrid process (PCHP) that has been developed and put into practical use. When using this technology for the glass melting furnace exhaust gas treatment, it is essential that the glass production equipment, the existing De-SO_x, and the dust collection equipment are not affected during normal operations. Therefore, a small-scale laboratory experiment was carried out prior to the actual equipment test. Based on the results, we incorporated the technology into the actual desulfurization facility of a glass melting furnace and conducted an experiment to demonstrate its practical use. This study elaborates on the current status of exhaust gas treatment in glass melting furnaces and explains the PCHP principle and the results obtained in actual system experiments.

II. Experiment with Exhaust Gas Treatment of Glass Manufacturing System

A. Glass Manufacturing System and Aftertreatment System

Figure 1 shows a schematic of the glass bottle manufacturing system and the dry exhaust gas treatment process. The raw materials of glass such as silica sand, limestone, soda ash, sodium sulfate (Na_2SO_4), etc. are melted in a glass melting furnace at approximately 1500°C using a fossil fuel such as city gas or C-heavy oil. Because of technical issues of glass melting, the furnace cannot be used for city gas firing alone. C-heavy oil is used at a ratio of approximately 1/4–1/3, which results in SO_x generation. In a bottle manufacturing system, the melted glass is transformed into a bottle shape using a mold and then it is slowly cooled for distortion removal. Subsequently, it is used to develop a glass bottle product. However, the exhaust gas emitted by combustion contains air pollutants such as SO_x derived from raw materials and fuels, NO_x generated by high-temperature air combustion, and dust (mainly scattered materials). Therefore, exhaust gas treatment facilities are installed to reduce environmentally hazardous substances. The exhaust gas from the glass melting furnace passes through a thermal storage apparatus and is introduced into a downstream reaction tower called a stabilizer or a reactor. In this reaction tower, an aqueous solution of sodium hydroxide (NaOH) is sprayed, and SO_x in the exhaust gas is removed. The removed SO_x is

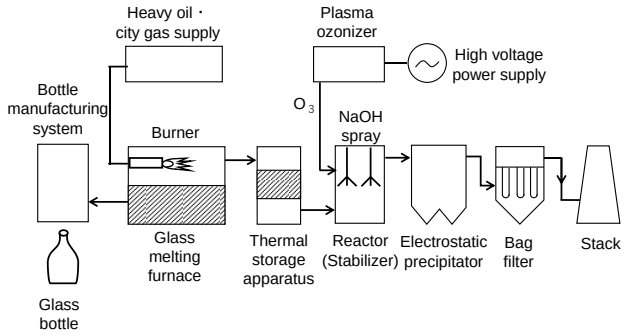

Fig. 1. Schematic of glass bottle manufacturing system and dry exhaust gas treatment system.

converted to sodium sulfite (Na_2SO_3), which is oxidized and recovered as Na_2SO_4 and reused as a glass raw material. The generated fine particles of Na_2SO_4 and dust are removed by a dry EP and a BF, which are located downstream and are used as dust collectors. The dust is transported to the glass melting furnace by a chain conveyor. The cleaned exhaust gas is discharged from the stack. However, because the exhaust gas contains a large amount of sticky dust produced by raw materials and high-concentration SO_x, De-NO_x equipment has not been able to improve. NO_x regulations (NO_x < 350 ppm at O_2 = 15%) have been complied with by the reduction of NO_x due to low air ratio combustion at the source side. However, because NO_x reduction in low air ratio combustion is accompanied by a deterioration in fuel efficiency, the demand for energy-saving NO_x reduction technology has increased.

The specification of the glass melting furnace is listed in **Table 1**.

Table 1. Specification of glass melting furnace.

Items	Specification
Type	Side-port-type glass melting furnace
Thermal output	10 MW class
Fuels	City gas and C-heavy oil
Burner type	Diffusion combustion burner
Flow rate of flue gas	32127 Nm^3/h (dry) (rating value)
Glass production rate	233 ton/day (maximum value)

Therefore, we developed PCHP technology for a glass melting furnace that performs De-NO_x by injecting ozone gas generated by the plasma ozonizer into the reaction tower while cooling the gas with water. The De-NO_x reactions are given as reactions (1)–(3).

$$O_3 \rightarrow O_2 + O \quad (1)$$

$$NO + O \rightarrow NO_2 \quad (2)$$

$$2NO_2 + 4Na_2SO_3 \rightarrow N_2 + 4Na_2SO_4 \quad (3)$$

Ozone is injected into the flue gas. According to reaction (1), ozone is thermally decomposed to form the O radical. In reaction (2), the NO in the exhaust gas is oxidized to NO_2. Hydroxyl radical (–OH) could be induced by the reaction between O_3 and water to enhance the NO oxidation. In reaction (3), NO_2 reacts with Na_2SO_3 to produce Na_2SO_4; These reactions help in achieving complete purification. Furthermore, Na_2SO_4 can be reused as a glass raw material in the furnace. In reaction (4), Na_2SO_3 is obtained as a reducing agent between NaOH in the stabilizer and SO_2 in the exhaust gas.

$$SO_2 + 2NaOH \rightarrow Na_2SO_3 + H_2O \quad (4)$$

B. Plasma Ozonizer

The specifications of the ozonizers are listed in **Table 2**. Two sets of plasma-type ozonizers (ozone yields of 4 and 6 kg/h) are used simultaneously in the pilot scale demonstration test. Both are dielectric barrier discharge ozonizers, which use an oxygen tank as the oxygen supply source. Each unit has 300–400 nonthermal plasma reactors. In this demonstration test, two sets of ozonizers are used simultaneously to inject ozone into the reactor. The maximum concentration of ozone generated is 7.0% (= 150 g/Nm^3) and the mass flow rate is 10.0 kg/h at a maximum power consumption of 28 + 48 = 76 kW. The thermal input for the furnace is 10 MW, whereas input power to the plasma ozonizer is 76 kW, which is a small portion of 0.8% of the thermal input, because plasma ozonizer acts efficiently and is only used for the oxidation of NO to NO_2. NO_2 reduction to N_2 is performed using the chemical process in the PCHP. The structure of a single nonthermal plasma reactor uses the dielectric barrier type shown in **Fig. 2**. It consists of a glass dielectric, a centered electrode covered with dielectric material, and a grounded electrode cooled with cooling water. The total flow rate of oxygen is 26.7 and 40.0 Nm^3/h for the 4.0 and 6.0 kg/h ozonizers, respectively.

Table 2. Specification of ozonizers.

Item	Specification	
Manufacturer	Sumitomo Precision Products Co., Ltd.	
Type	SAGT4M-C	SAGT6M-C
Plasma type	Dielectric barrier discharge with water-cooled electrodes	
Number of interior glass plasma reactors	334	432
Discharge voltage	5 kV	5 kV
Maximum ozone generation rate	4.0 kg/h	6.0 kg/h
Ozone concentration	150 g/Nm^3 = 7.0%	
Oxygen pressure at the inlet	0.13 MPa (gauge)	
Oxygen flow rate at the inlet	26.7 Nm^3/h	40.0 Nm^3/h
Oxygen pressure at the inlet	~0.12 MPa (gauge)	
Flow rate of cooling water	102 L/min	153 L/min
Temperature of cooling water at the inlet	15 °C at the inlet (temperature difference is approximately 5°C)	
Width of ozone generation control	10–100% of the maximum generation	
Power consumption	28 kW	48 kW
Power source	AC 400 V, three-phase, 50 Hz	

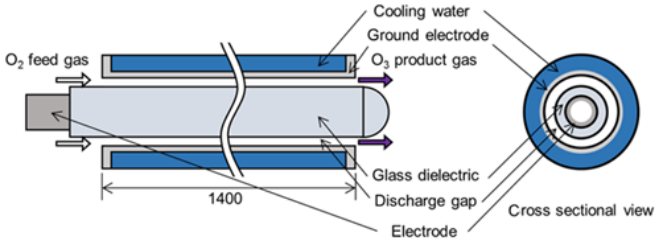

Fig. 2. Structure of a single nonthermal plasma reactor in the ozonizers.

C. Experimental Results and Discussion

For a glass melting furnace, a semi-dry De-SO_x apparatus is used more frequently as an exhaust gas treatment device than the wet type, especially in the developing countries. The reason for this is that the wet treatment eventually requires the treatment of wastewater, and the white smoke discharge from the stack due to water vapor may cause environmental problems. This is the reason why the dry type in which the exhaust gas is completely dried is preferred. Therefore, a dry pilot-scale plant that incorporates PCHP into a semi-dry De-SO_x unit of a glass melting furnace was constructed by Nihon Yamamura Glass Co., Ltd, as shown in **Fig. 1**. The plant was built in their Tokyo factory, and simultaneous dry De-SO_x and De-NO_x testing are performed with an exhaust gas volume (~18450 Nm^3/h). Moreover, in this glass melting furnace, the combustion is performed by switching a pair of regenerators and burners at fixed time intervals. In this case, Na_2SO_3 produced by the process of reaction (4) in the reaction tower or Na_2SO_4 by air oxidation becomes particulate and is collected by the downstream EP. It is necessary to maintain the temperature of the exhaust gas at the outlet of the reaction tower in the range of 200 to 250°C to prevent a decrease in dust collection efficiency in a wet state. Therefore, it is necessary to maintain the spray amount of the NaOH aqueous solution low.

Previous studies showed that when the exhaust gas temperature exceeds 150°C, the NO oxidation performance due to O_3 injection decreases. Hence, there is a need for the reduction of NO oxidation even for averaged high-temperature exhaust gas exceeding 150°C. For this reason, it is important to efficiently supply ozone to the local cooling area containing spray droplets formed by water spray below 150°C, and the ozone spray nozzle should be directed towards the center of the cooling area. It was confirmed that the outlet temperature of the reaction tower could be maintained at 200°C or higher while the local cooling area was kept cooled to approximately 70°C with NaOH aqueous solution.

Exhaust gas discharged from the glass melting furnace is first introduced into a semi-dry desulfurization unit (reaction tower). The reactor is a cylindrical De-SO_x tower having a diameter of 3.5 m and a height of 21.5 m. Air, cooling water, and ozone gas are simultaneously sprayed by a three-fluid nozzle (manufactured by H. IKEUCHI & Co., Ltd.) installed 2.05 m above the inlet of the reaction tower to oxidize NO. Next, a two-fluid nozzle (manufactured by H. IKEUCHI & Co., Ltd.) is installed 4.05 m above the inlet of the reaction tower, and NO_x and SO_x were simultaneously treated by spraying NaOH solution. The dried exhaust gas from the outlet of the reaction tower then passes through the dry EP and the BF to remove PM and then is discharged to the atmosphere.

Figures 3 and **4** show the NO and NO_x measurement results. In the figures, O_2 = 15% equivalent values are shown for NO and NO_x. ΔNO and ΔNO_x are NO and NO_x removals, respectively. The oxygen supplied to the reactor via the three-fluid nozzle dilutes the gas and oxygen concentration slightly increases. Because De-NO_x and De-SO_x were evaluated based on O_2 of 15% equivalent concentrations, there is no effect of it. Experiments are performed under three conditions. In 2–T1, the ozone injection rate is 0 kg/h; in 2–T2, the ozone injection rate is 5.9 kg/h; in 2–T3, the ozone injection rate is 4.0 kg/h. The experiment is performed for 6 hrs. To satisfy the regulation of NO_x emission, combustion adjustment with a lower air ratio (λ < 1.0) has been carried out in the factory, resulting in lower combustion efficiency and increased CO and soot generation. In the experiment, higher air ratio (λ = 1.1) with PCHP aftertreatment is used, resulting in energy-saving operation while satisfying the regulation requirements. The average value at the reaction tower temperature measurement point of z = 2.85 m above the reaction tower inlet (NO oxidation area) is approximately 90°C, and a sufficient local cooling area is formed. The average NO_x removal efficiency is 0% for 2–T1, 16% for 2–T2, and 6.4% for 2–T3. The average NO_x removal efficiency is the highest under the condition of 2–T2. When the ozone injection amount increases, the NO_x removal rate tended to increase. From the above-mentioned experiments that were conducted at real machine scale, we succeeded in securing a sufficient cooling area by increasing the spray amount. As a result, satisfactory De-NO_x are obtained.

Figure 5 shows the SO_2 measurement result. In the Air Pollution Control Act of Japan, a k value regulation is valid for SO_x emission from factories: $q < k \times 10^{-3} \times H_e^2$, where q is the allowable emission of sulfur oxides (Nm^3/h), k is the coefficient determined by region, and H_e is the effective height of stack (m). Because k = 11.5 and H_e = 60.3 m for the factory, q should be less than 41.82 Nm^3/h, which corresponds to SO_2 < 1093 ppm (O_2 = 15%). Furthermore, more stringent regional regulation of Kanagawa Prefecture is determined as q < 37.11 Nm^3/h and SO_2 < 970 ppm (O_2 = 15%). The emission in **Fig. 5** fully satisfies these regulations. Furthermore, SO_2 removal is enhanced and ΔSO_2 = 200 ppm is realized when the plasma is turned on.

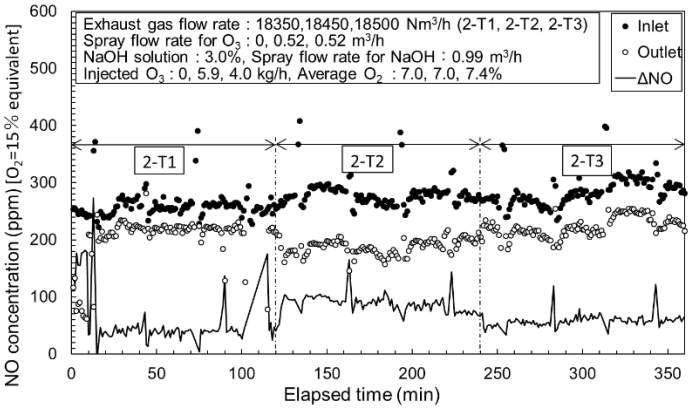

Fig. 3. Time-dependent NO measurement result.

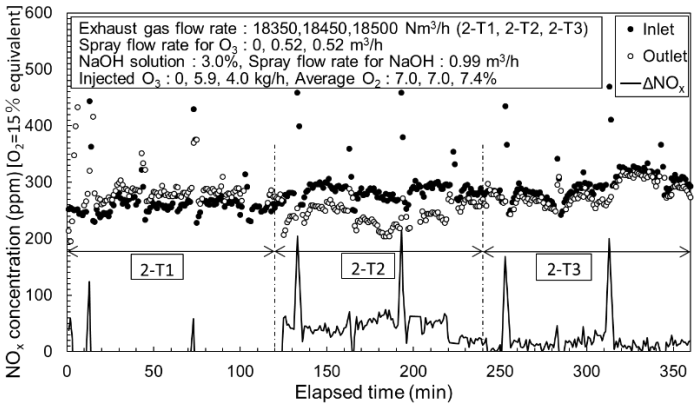

Fig. 4. Time-dependent NO_x measurement result.

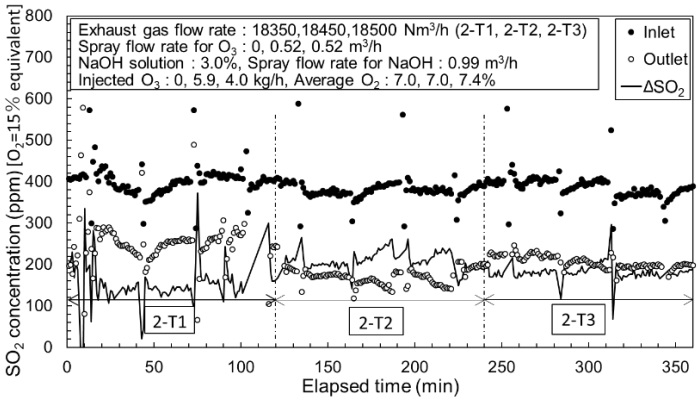

Fig. 5. Time-dependent SO_2 measurement result.

It is confirmed that dry De-SO_x and De-NO_x of glass melting furnace exhaust gas with PCHP is possible. High removal efficiencies for NO, NO_x, and SO_x of 33, 16, and 56%, respectively, are obtained for the 2-T2 test. The energy efficiency of NO_x removal obtained by evaluating the electrical power using the cost of NaOH and the power consumption of ozonizers in the 2-T2 test is 23 g(NO_2)/kWh. It is noted that the NO_x removal efficiency appears to be not very efficient. More optimal operations and a larger amount of O_3 injection should be realized to get higher NO_x and SO_x removal efficiencies.

III. Result of Numerical Prediction

A. Numerical Method

A numerical design was used for the prediction of the system. Numerical simulation was carried out inside the two-phase chemical reaction flow of the stabilizer. O_3 is injected before the gas passes through the stabilizer. **Figure 6** shows the analysis model. The simulated exhaust gas flows from the pipe (z = 0 mm) connected to the reactor (stabilizer). Water is then sprayed from a three-fluid nozzle installed at a position of z = 2050 mm and a two-fluid nozzle installed at a position of z = 4050 mm to form a local cooling area in the reactor. Further, ozone is ejected from the three-fluid nozzle to oxidize NO in the simulated exhaust gas. The treated simulated exhaust gas flows out through the pipe (z = 14900 mm) connected to the upper part of the reactor. The gas does not flow out from the bottom of the reactor (z = –4900 mm). Heat dissipation and non-slip conditions at wall boundaries are used as boundary conditions. A steady three-dimensional simulation is performed using the finite volume method. CFD-ACE+ (CFD-ACE-GUI version 2020.5.0, ESI Group) was used as the simulation software.

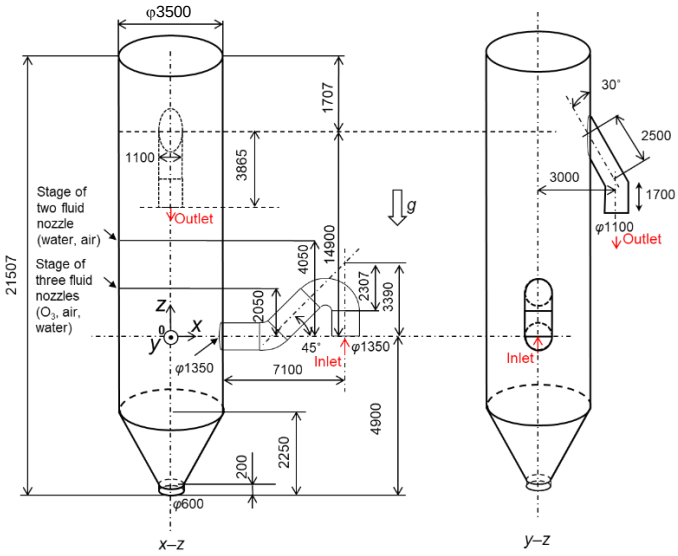

Fig. 6. 3D analysis model for the stabilizer.

B. Governing Equation

A simulation that combines the thermal fluid flow of gas-phase including chemical reactions with the thermal motion of water droplets considering evaporation is performed. The governing equations for a three-dimensional compressible steady-state gas-phase problem can be described as follows.

Continuity equation:

$$\nabla \cdot (\rho \boldsymbol{u}) = M_{\mathrm{d}} \tag{5}$$

Momentum equation:

$$\nabla \cdot (\rho \boldsymbol{u}\boldsymbol{u}) = -\nabla p + \nabla \cdot (\mu \nabla \boldsymbol{u}) + \rho \boldsymbol{g} + \boldsymbol{f}_{\mathrm{d}} \tag{6}$$

where ρ, $\boldsymbol{u}$, M_{d}, p, μ, $\boldsymbol{g}$, and $\boldsymbol{f}_{\mathrm{d}}$ are the fluid density, fluid velocity vector, evaporation rate of water droplets per volume, pressure, viscosity, gravitational acceleration, and body force by water droplets, respectively.

Equation of state:

$$p = \rho R T \tag{7}$$

Energy equation:

$$\nabla \cdot (\rho \boldsymbol{u} h) = \nabla \cdot (\lambda \nabla T) + \psi_{\mathrm{D}} + S_{\mathrm{C}} + S_{\mathrm{d}} \tag{8}$$

where R, T, h, λ, Ψ_D, S_C, and S_d are the gas constant, absolute temperature, total enthalpy, thermal conductivity, dissipation loss, heat source of chemical reactions, and heat source of water droplets, respectively.

The transport equations of chemical species i are expressed as

$$\nabla \cdot \left(\rho \boldsymbol{u} Y_i \right) = \nabla \cdot \boldsymbol{J}_i + M_i \omega_i \tag{9}$$

where Y_i, $\boldsymbol{J}_i$, M_i, and ω_i are the mass fraction, mass flux, molecular weight, and molar production rate, respectively. The mass flux, $\boldsymbol{J}_i$, is given as

$$\boldsymbol{J}_i = -\rho D_i \nabla Y_i + \rho Y_i \boldsymbol{u}_{di} + \boldsymbol{J}_{ci} \tag{10}$$

where D_i (= $\mu/(\rho Sc)$) is the diffusion coefficient, and $\boldsymbol{u}_{di}$ and $\boldsymbol{J}_{ci}$ are the drift velocity and mass flux, respectively, which are generated because of the Stefan–Maxwell procedure to satisfy mass conservation. In this study, the re-normalization group k–ε model is used as the turbulence model to manage the rapid changes in the flow field caused by droplet spray. Linear and logarithmic laws are used as wall functions in the viscous and inertial layers, respectively.

For the calculation of the thermal motion of spraying water droplets, the discrete particle method is simulated in the computational domain by solving the Lagrange equation. For the evaporation model, a water droplet is considered spherical and the temperature distribution inside the droplet is considered uniform without considering the circulation inside the droplet. The equation of motion of the droplet is expressed as follows:

$$m_i \frac{\mathrm{d}\boldsymbol{v}_i}{\mathrm{d}t} = C_D \rho_d \left(\boldsymbol{u} - \boldsymbol{v}_i \right) \left| \boldsymbol{u} - \boldsymbol{v}_i \right| \frac{A_i}{2} + m_i \boldsymbol{g} \tag{11}$$

where i, m, C_D, ρ_d, $\boldsymbol{v}$, and A are the droplet number, droplet mass, drag coefficient, droplet density, droplet velocity, and droplet projection surface area, respectively. The first term on the right side is the drag force that a single water droplet receives from the gas. The reaction force of the drag force, integrated over the number of droplets in one cell in Cartesian coordinates, is the drag force, $\boldsymbol{f}_d$, that the gas receives. When a water droplet moves through gas at a high temperature, the droplet evaporates, and energy is exchanged. The energy equation for a droplet is expressed as follows:

$$m_i C_p \frac{\mathrm{d}T_i}{\mathrm{d}t} = \pi d^2 s - \dot{m}_{eva} L \tag{12}$$

where C_p, s, d, $\dot{m}_{eva}$, and L are the specific heat of the droplet, sensible heat transferred to the droplet, diameter of the droplet, evaporation rate of the droplet, and latent heat, respectively.

The water droplet diameter, d, which decreases with evaporation, is expressed as follows:

$$\frac{\mathrm{d}\left(d_0^3 - d^3 \right)}{\mathrm{d}t} = \frac{6}{\pi \rho_d} \dot{m}_{eva} \tag{13}$$

where subscript 0 denotes the start of the simulation iteration. The gas, density, velocity, temperature, pressure, and concentration of the species are obtained using Equations (5)–(10); the droplet trajectory, diameter, velocity, and temperature are obtained using Equations (11)–(13).

Table 3 lists the five equations of chemical reactions [26] that are used considering the NO oxidation and ozone decomposition. Reaction rate constants are expressed as $k = AT^n \exp(-E/R/T)$, and R = 8.31446 kJ/K/mol. It is noted that liquid phase reactions are not considered.

Table 3. Chemical reactions and rate constants considered.

Reactions	A, cm^3/mol/s	n	E, kJ	E/R, K
$NO + O_3 \rightarrow NO_2 + O_2$	2.59×10^{12}	0	13.3	1.60×10^{3}
$NO + O \rightarrow NO_2$	2.83×10^{13}	0	1.10	1.32×10^{2}
$N_2 + 2O \rightarrow N_2 + O_2$	8.81×10^{13}	0	–6.30	7.58×10^{2}
$O_3 \rightarrow O_2 + O$	4.31×10^{14}	0	92.95	1.12×10^{4}
$O_3 + O \rightarrow 2O_2$	6.32×10^{11}	0	18.04	2.17×10^{3}

In the experiment, the inner diameter of the spray hole of the three-fluid nozzle is 15 mm and the number of a hole is one, and 2 mm for the two-fluid nozzle and the number of a hole is six. The average size (Sauter mean diameter) of the water spray droplets sprayed from the three-fluid nozzles is 20 to 100 μm, and the maximum is approximately 140 μm. The average size (Sauter mean diameter) of the NaOH solution spray droplets sprayed from the two-fluid nozzles is 50 to 100 μm and the maximum is approximately 200 μm. In the simulation, the spray droplets of both nozzles are set to be the lognormal distributions for the constant diameters of 50, 100, and 140 μm with the average diameter of 100 μm. From the viewpoint of computational load, the maximum average diameter value 100 μm of the average size range in the experiment is applied to the simulation.

C. Numerical Prediction Results

Figure 7 shows the temperature distribution. It is found that the simulated exhaust gas flows in at 488°C, is cooled by water spray from the three-fluid nozzle and the two-fluid nozzle, and flows out of the outlet at 260°C. The exhaust gas flows out in a dry state due to the high temperature of 260°C. At a position of z = 2050 mm (where the three fluid nozzles are mounted), a local cooling area is formed, and the simulated exhaust gas is cooled to a minimum temperature of 60°C. Even at the spray position of z = 4050 mm (where the two-fluid nozzles are mounted), a local cooling area is still formed, and the gas is cooled to a minimum temperature of 100°C. It is also found that the simulated exhaust gas density increases with the decrease in the temperature so that a cooling region extends to the upstream (z = 1000 mm) from the spray position of the first stage.

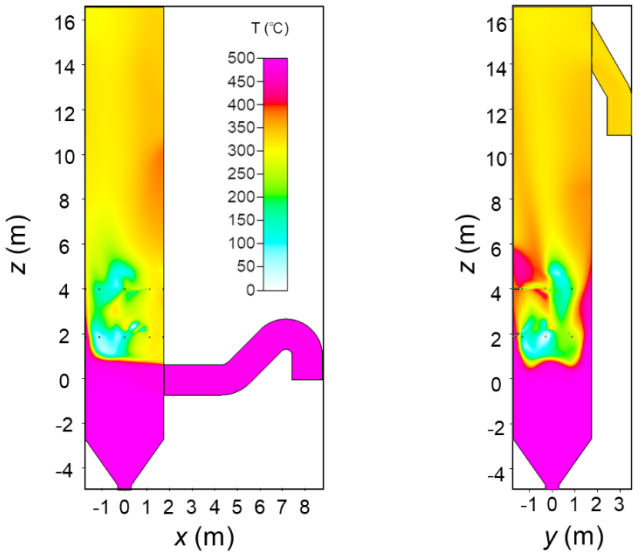

(a) (b)

Fig. 7. Temperature distributions of gaseous phase, (a) *x*–*z* cross section (b) *y*–*z* cross section.

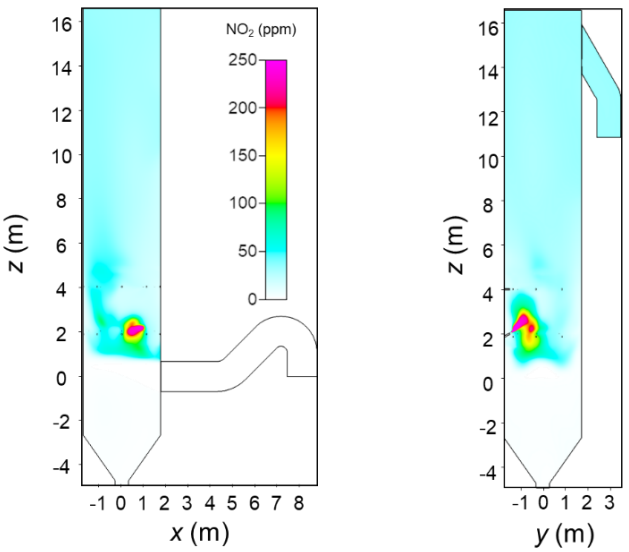

(a) (b)

Fig. 9. NO_2 concentrations, (a) *x*–*z* cross section (b) *y*–*z* cross section.

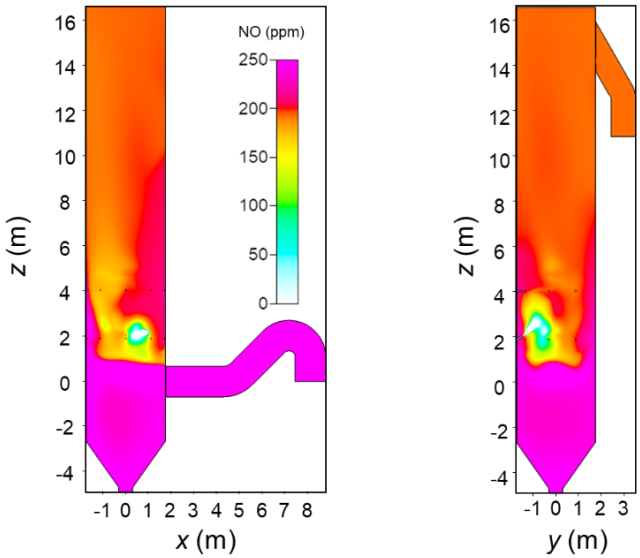

(a) (b)

Fig. 8. NO concentrations, (a) *x*–*z* cross section (b) *y*–*z* cross section.

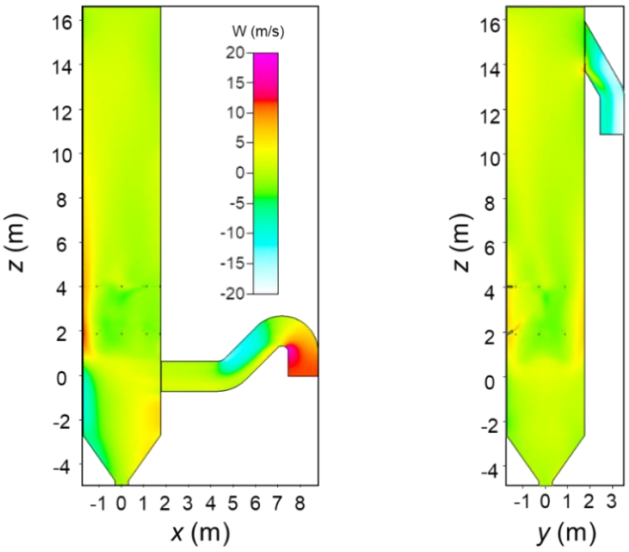

(a) (b)

Fig. 10. Counter of velocity in the *z* direction, (a) *x*–*z* cross section (b) *y*–*z* cross section.

Figures 8 and **9** show the NO and NO_2 distribution, respectively. NO_2 is generated near the outlet of the three-fluid nozzle and reaches a local concentration of around 30 ppm at the exit of the stabilizer. The concentration of NO_2 agree well with the measurement results in **Fig. 4**. After NO_2 is generated near the nozzle, it flows to the lower region (z = 800 mm) of the three-fluid nozzle and then disperses downstream. The region where the NO_2 is generated and dispersed agrees well with the cooling region.

Figure 10 shows v_z or w distribution. A strong upward flow near the wall (x < –1750 mm) is obtained. This is caused by the flow from the inlet colliding with the wall. The upward flow near the walls are also confirmed. This is due to the large vortex created by the convection of the simulated exhaust gas cooled by the three-fluid and two-fluid nozzles. It is found that NO_2 is diffused by the convection field generated by the cooling and advects by the upward flow.

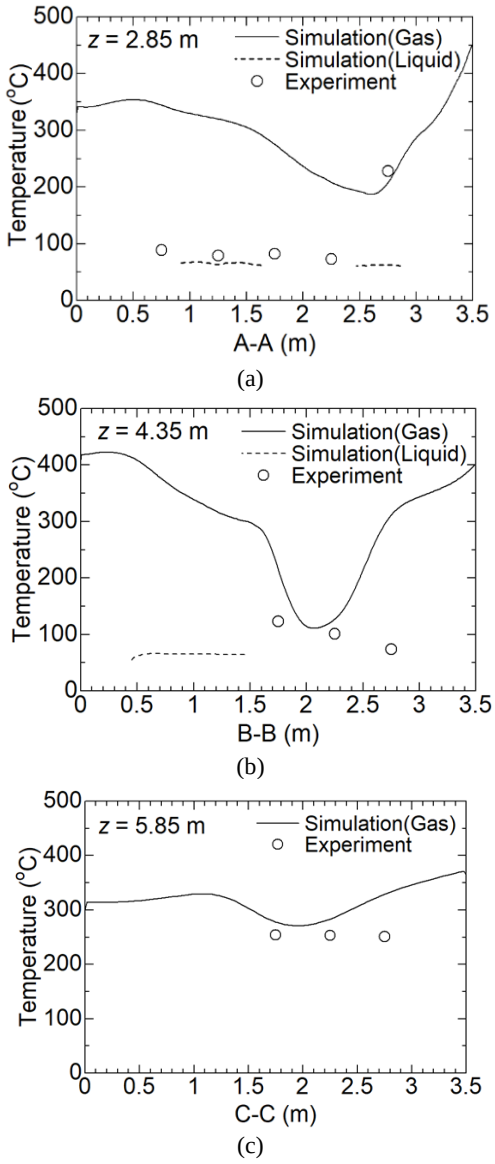

Fig. 11. Comparison of simulated and experimental temperature distributions, (a) z = 2.85 m (b) z = 4.35 m (c) z = 5.85 m.

Figure 11 shows a comparison of simulated and experimental temperature distributions. In all the figures, calculated gas-phase and liquid-phase temperatures are shown with solid curves and broken curves, respectively, when liquid phase exists at A-A, B-B, and C-C lines. Further, the measured data obtained via thermocouples are indicated using circles. It is believed that the liquid phase temperatures can be measured at the gas liquid two phase position, and the gas-phase temperatures can be measured at the gas single phase position. The results show that there is good agreement between them.

From these results in **Fig. 11**, it can be concluded that numerical design simulation provides a satisfactory result. To improve the accuracy of numerical calculations, it is possible to carry out unsteady simulations, considering detailed water droplet particle size distributions and more chemical equations including NO_2 reduction reactions.

IV. Concluding Remarks

In this study, as an application example for plasma chemical hybrid exhaust gas treatment technology, we elaborated on the current status of glass melting furnace exhaust gas treatment, and the results obtained in actual machine tests. Furthermore, a numerical design was presented for the technology. PCHP can be considered as the most suitable method for exhaust gas treatment in glass melting furnaces because it can maintain the degree of De-NO_x and De-SO_x of exhaust gas while reusing SO_x in the exhaust gas as a glass material using reaction (3). More optimal operations and a larger amount of O_3 injection should be realized to get higher NO_x and SO_x removal efficiencies. The company and the university jointly plan to continue further research to improve De-NO_x efficiency in dry processes. Ultimately, we hope to expand the application of this exhaust gas treatment method to glass melting furnaces around the world.

Acknowledgments

We are grateful to R. Tsuji, K. Yamakawa (Nihon Yamamura Glass Co., Ltd.), K. Maeda, Y. Mizuguchi, and R. Nishioka (graduate students at Osaka Prefecture University) for their cooperation during the experiments. Furthermore, this study is subsidized by a project fund (Strategic Innovation Program for Energy Conservation Technologies: JPNP12004) of the New Energy and Industrial Technology Development Organization (NEDO).

References

[1] M. Okubo and T. Kuwahara (2019) New technologies for emission control in marine diesel engines. Butterworth-Heinemann, imprint of Elsevier, Paperback ISBN: 9780128123072, page count: 296.

[2] M. Okubo (2021) Recent development of technology in scale-up of plasma reactors for environmental and energy applications, Plasma Chem. Plasma P., https://doi.org/10.1007/s11090-021-10201-7.

[3] H. Fujishima, K. Takekoshi, T. Kuroki, A. Tanaka, K. Otsuka, and M. Okubo (2013) Towards ideal NO_x control technology for bio-oils and a gas multi-fuel boiler system using a plasma-chemical hybrid process. Appl Energy 111:394–400.

[4] H. Fujishima, Y. Yoshioka, T. Kuroki, A. Tanaka, K. Otsuka, and M. Okubo (2011) Development of low-emission bio-fuel boiler system with plasma-chemical hybrid NO_x reduction. IEEE Trans Ind Appl 47:2210–2217.

[5] H. Fujishima, A. Tatsumi, T. Kuroki, A. Tanaka, K. Otsuka, T. Yamamoto, and M. Okubo (2010) Improvement in NO_x removal performance of the pilot-scale boiler emission control system using an indirect plasma chemical process. IEEE Trans Ind Appl 46:1722–1729.

[6] H. Fujishima, T. Kuroki, T. Ito, K. Otsuka, T. Yamamoto, K. Yoshida, and M. Okubo (2010) Performance characteristics of pilot-scale indirect plasma and chemical system used for the removal of NO_x from boiler emission. IEEE Trans Ind Appl 46:1707–1714.

[7] M. Yasuda, N. Tsugita, K. Iubto, S. Yamauchi, W. R. Glomm, I. Tsuji, and H. Asano (2011) High-efficiency NO_x absorption in water using equipment packed with a glass fiber filter. Environ Sci Technol 45:1840–1846.

[8] T. Kuwahara, K. Yoshida, T. Kuroki, K. Hanamoto, K. Sato, and M. Okubo (2019) High reduction efficiencies of adsorbed NO_x in pilot-scale aftertreatment using nonthermal plasma in marine diesel-engine exhaust gas. Energies 12:3800.
[9] T. Kuwahara, K. Yoshida, T. Kuroki, K. Hanamoto, K. Sato, and M. Okubo (2020) Pilot-scale combined reduction of accumulated particulate matter and NO_x using nonthermal plasma for marine diesel engine. IEEE Trans Ind Appl 56:1804–1814.
[10] M. Hołub, S. Kalisiak, T. Borkowski, J. Myśków, and R. Brandenburg (2010) The influence of direct non-thermal plasma treatment on particulate matter (PM) and NO_x in the exhaust of marine diesel engines. Polish J of Environ Stud 19:1199–1211.
[11] W. Balachandran, N. Manivannan, R. Beleca, and M. Abbod (2015) Reduction of NO_x and PM in marine diesel engine exhaust gas using microwave plasma. J Phys Conf Ser 646, 012053.
[12] W. Balachandran, N. Manivannan, R. Beleca, M. Abbod, D. Brennen, N. S. Alozie, and L. C. Ganippa (2016) Nonthermal plasma system for marine diesel engine emission control. IEEE Trans Ind Appl 52:2496–2505.
[13] T. Kuwahara, K. Yoshida, T. Kuroki, K. Hanamoto, K. Sato, and M. Okubo (2020) Pilot-scale combined reduction of accumulated particulate matter and NO_x using nonthermal plasma for marine diesel engine. IEEE Trans Ind Appl 56:1804–1814.
[14] T. Kuwahara, K. Yoshida, K. Hanamoto, K. Sato, T. Kuroki, and M. Okubo (2015) A pilot-scale experiment for total marine diesel emission control using ozone injection and nonthermal plasma reduction. IEEE Trans Ind Appl 51:1168–1178.
[15] T. Kuwahara, K. Yoshida, K. Hanamoto, K. Sato, T. Kuroki, T. Yamamoto, and M. Okubo (2012) Pilot-scale experiments of continuous regeneration of ceramic diesel particulate filter in marine diesel engine using nonthermal plasma-induced radicals. IEEE Tran Ind Appl 48:1649–1656.
[16] R. Fan, Y. Cai, Y. Shi, and Y. Cui (2019) Effect of the reaction temperature on the removal of diesel particulate matter by ozone injection. Plasma Chem Plasma Process 39:143–163.
[17] D. Lee, H. Kim, Y. -H. Song, and K. -T. Kim (2014) Plasma burner for active regeneration of diesel particulate filter. Plasma Chem Plasma Process 34:159–173.
[18] M. Higashi, S. Uchida, N. Suzuki, and K. Fujii (1992) Soot elimination and NO_x and SO_x reduction in diesel-engine exhaust by a combination of discharge plasma and oil dynamics. IEEE Trans Plasma Sci 20:1–12.
[19] C. Fushimi, K. Madokoro, S. Yao, Y. Fujioka, and K. Yamada (2008) Influence of polarity and rise time of pulse voltage waveforms on diesel particulate matter removal using an uneven dielectric barrier discharge reactor. Plasma Chem Plasma Process 28:511–522.
[20] J. Zhu, Q. Zhao, Y. Yao, S. Luo, X. Guo, X. Zhang, Y. Zeng, and K. Yan (2012) Effects of high-voltage power sources on fine particle collection efficiency with an industrial electrostatic precipitator. J Electrostat 70:285–291.
[21] S. Ma, Y. Zhao, J. Yang, S. Zhang, J. Zhang, and C. Zheng (2017) Research progress of pollutants removal from coal-fired flue gas using non-thermal plasma. Renewable Sustainable Ener Rev 67:791–810.
[22] J. S. Chang, K. Urashima, Y. X. Tong, W. P. Liu, H. Y. Wei, F. M. Yang, and X. J. Liu (2003) Simultaneous removal of NO_x and SO_2 from coal boiler flue gases by DC corona discharge ammonia radical shower systems: Pilot plant tests. J Electrostat 57:313–323.
[23] B. Han, H. J. Kim, and Y. J. Kim (2015) Removal of NO and SO_2 in a cylindrical water-film pulse corona discharger. IEEE Trans Ind Appl 51:679–684.
[24] S. Li, Y. Huang, F. Wang, J. Liu, F. Feng, X. Shen, Q. Zheng, Z. Liu, L. Wang, and K. Yan (2014) Fundamentals and environmental applications of non-thermal plasmas: multi-pollutants emission control from coal-fired flue gas. Plasma Chem Plasma Process 34:579–603.
[25] Y. -H. Lee, W. -S. Jung, Y. -R Choi, J. -S Oh, S. -D Jang, Y. -G. Son, M. -H Cho, W. Namkung, D. -J. Koh, Y. -S. Mok, and J. -W. Chung (2003) Application of pulsed corona induced plasma chemical process to an industrial incinerator. Environ Sci Technol 37:2563–2567.
[26] Y. S. Mok, and H. J. Lee (2006) Removal of sulfur dioxide and nitrogen oxides by using ozone injection and absorption–reduction technique. Fuel Process Technol 87:591–597.
[27] H. Yamamoto, T. Kuroki, H. Fujishima, and M. Okubo (2016) Pilot-scale exhaust gas treatment for a glass manufacturing system using a plasma combined wet chemical process, Mechanical Engineering J. 3, 15-00549-15-00549 (2016).
[28] H. Yamamoto, T. Kuroki, H. Fujishima, and M. Okubo (2019) Pilot-scale NO_x and SO_x aftertreatment using a two-phase ozone and chemical injection in glass-melting-furnace exhaust gas. IEEE Trans Ind Appl 55:6295–6302.
[29] H. Yamasaki, Y. Mizuguchi, R. Nishioka, Y. Fukuda, T. Kuroki, H. Yamamoto, and M. Okubo (2021) Pilot-scale NO_x and SO_x aftertreatment by semi-dry plasma-chemical hybrid process in glass-melting-furnace exhaust gas. Plasma Chem Plasma P. https://doi.org/10.1007/s11090-021-10193-4.
[30] H. Yamasaki H. Yamamoto, Y. Koizumi, Y. Fukuda, T. Kuroki, and M. Okubo, Dry emission control technology for glass melting furnace by plasma-chemical hybrid processing, Proc. 2021 IEEE Industry Applications Society Annual Meeting, October 10th–14th, 2021.
[31] S. J. Schmieg (2010) Aspects of HC-SCR catalyst durability for lean-burn engine exhaust aftertreatment. SAE Paper 2010-01-2160.
[32] M. Masui, Y. Hayakawa, A. Takeyama, T. Miura, and S. Kambara (2014) Low temperature SNCR tests by injection of activated ammonia generated by DBD. Proc. of the ISEHD 2014 Okinawa, Japan.
[33] Y. Hayakawa, Y. Inoue, A. Takeyama, and S. Kambara (2016) Reaction mechanism of De-NO_x by activated ammonia generated by dielectric barrier discharge. Int J Plasma Environmental Sci & Tech 10:20–23.

Haruhiko Yamasaki (M'20) received his B. Eng., M. Eng., and Ph. D. degrees in mechanical engineering from Doshisha University, in 2011, 2013, and 2016, respectively. He is currently an Assistant Professor at the Department of Mechanical Engineering at Osaka Metropolitan University. He is currently carrying out a study on the development of nonthermal plasma applications for air pollution control and indoor air cleaning.

Dr. Yamasaki is a member of the IEEE Industry Application Society, Japan Society of Mechanical Engineers, and Institute of Electrostatics, Japan.

Hashira Yamamoto was born in Osaka Prefecture, Japan, in 1978. He received the B. Eng. and M. Eng. degrees in chemical engineering from Kansai University, Osaka, Japan in 2001 and 2003, respectively, and the Ph. D. degree in mechanical engineering from Osaka Prefecture University, Osaka, Japan, in 2017. He belongs to the Environmental Affairs Office of Nihon Yamamura Glass Co., Ltd., and he is a Visiting Research Fellow with the Department of Mechanical Engineering, Osaka Metropolitan University. His research interests include nonthermal plasma and chemical processes for the NO_x and SO_x emission control of glass manufacturing systems, and glass resource recycling. Dr. Yamamoto is a member of the Japan Society of Mechanical Engineers, and the Institute of Electrostatics Japan.

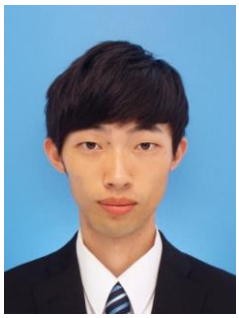

Yuki Koizumi received his B. Eng. and M. Eng. degrees in mechanical engineering from Osaka Prefecture University in 2019 and 2021, respectively. After graduation, he is working at Kawasaki Heavy Industries, Ltd., Kobe, Japan. He was involved in this research on dry emission control technology for glass melting furnace by plasma-chemical hybrid processing when he was a graduate student.

Yuta Fukuda received his B. Eng. and M. Eng. degrees in mechanical engineering from Osaka Prefecture University in 2020 and 2022, respectively. After graduation, he is working at Kubota Corporation, Osaka, Japan. He was involved in this research on dry emission control technology for glass melting furnace by plasma-chemical hybrid processing when he was a graduate student.

Tomoyuki Kuroki (M'01) received his B. Eng., M. Eng., and Ph. D. degrees in energy systems engineering from Osaka Prefecture University, in 1998, 2000, and 2005, respectively. He is currently an Associate Professor at the Department of Mechanical Engineering at Osaka Metropolitan University. He has published more than 50 peer-reviewed papers. His current research interests are nonthermal plasma applications for air pollution control and indoor air cleaning, numerical simulations of plasma, and surface treatment of a fluorocarbon polymer using plasma graft-polymerization.

Dr. Kuroki is a member of the IEEE Industry Application Society, Japan Society of Mechanical Engineers, Institute of Electrostatics, Japan, and Japan Association of Aerosol Science and Technology.

Masaaki Okubo (M'01-SM'16-IEEE Fellow'23) received the B.Eng., M.Eng., and Ph.D. degrees in mechanical engineering from the Tokyo Institute of Technology, Tokyo, Japan, in 1985, 1987, and 1990, respectively. He is currently a Full Professor with the Department of Mechanical Engineering, Osaka Metropolitan University, Sakai, Japan. He has authored more than 230 peer-reviewed and invited papers in scientific journals and has authored 33 books. His research interests include environmental applications of nonthermal plasmas, particularly, nanoparticle control, electrostatic precipitators, the aftertreatment of clean diesel engines and combustors, and the surface treatment of materials and its industry applications. He works in the multidisciplinary areas of electrical, chemical, and mechanical engineering.

Dr. Okubo is a Fellow of the Japan Society of Mechanical Engineers. He was the Chairman of the Electrostatic Process Committee of the IEEE Industry Application Society during 2016–2018. He is an Associate Editor for the IEEE TRANSACTIONS ON INDUSTRY APPLICATIONS, the Kansai Branch Chair of the Institute of Electrostatics Japan and an Editorial Board Member of the Journal of Electrostatics